Phase-Locked Loops- A Broad Perspective

James A. Crawford jcrawford@siliconrfsystems.com
March 19, 2004

1 Introduction

Few topics in electrical engineering have demanded as much attention over the years as the phase-locked loop (PLL). The PLL is arguably one of the most important building blocks necessary for modern digital communications, whether in the RF radio portion of the hardware where it is used to synthesize pristine carrier signals, or in the baseband digital signal processing where it is often used for carrier- and time-recovery processing. The PLL topic is also intriguing because a thorough understanding of the concept embraces ingredients from many disciplines including RF design, digital design, continuous and discrete-time control systems, estimation theory and communication theory.

The PLL landscape is naturally divided into (i) low signal-to-noise ratio (SNR) applications like Costas carrier-recovery and time-recovery applications and (ii) high SNR applications like frequency synthesis. Each of these areas is further divided between (a) analog/ RF continuous-time implementations versus (b) digital discrete-time implementations. The different manifestations of the PLL concept require careful attention to different usage, analysis, design and implementation considerations.

With so many good tutorials about PLLs available on the Internet and elsewhere today, a theoretically unifying development will be presented in this article with the intention of providing a deepened understanding for this extremely pervasive concept.

2 Phase-Locked Loop Basics

The best way to develop a sound understanding of the phase-locked loop is to review the fundamental theories upon which this concept is based. One of the factors contributing to the longevity of the PLL is that relatively simple implementations can still lead to nearly optimal solutions and performance.

2.1 Some PLL History

"While recovering from an illness in 1665, Dutch astronomer and physicist Christiaan Huygens noticed something very odd. Two of the large pendulum clocks in his room were beating in unison, and would return to this synchronized pattern regardless of how they were started, stopped or otherwise disturbed.

An inventor who had patented the pendulum clock only eight years earlier, Huygens was understandably intrigued. He set out to investigate this phenomenon, and the records of his experiments were preserved in a letter to his father. Written in Latin, the letter provides what is

believed to be the first recorded example of the synchronized oscillator, a physical phenomena that has become increasingly important to physicists and engineers in modern times[1]." It should come as no surprise that modern researchers would later find that the behavior of such injection-locked oscillators can be closely modeled based upon PLL principles [6,7,8,9]. Anyone who has tried to co-locate RF oscillators running at different but nearly the same frequency has experienced how incredibly sensitive this coupling phenomenon is!

In 1840, Alexander Bain proposed a fax machine that used synchronized pendulums to scan an image at the transmitting end and send electrical impulses to a matching pendulum at the receiving end to reconstruct the image. The device, however, was never developed.

"The phase-lock concept as we know it today was originally described in a published work by de Bellescize in 1932 [1] but did not fall into widespread use until the era of television where it was used to synchronize horizontal and vertical video scans. One of the earliest patents showing the use of a phase-locked loop with a feedback divider for frequency synthesis appeared in 1970 [2]. The phase-locked loop concept is now used almost universally in many products ranging from citizens band radio to deep-space coherent receivers[2]."

2.2 PLL Terminology

A PLL consists of three basic components that appear in one form or another [4,5]:

1. Phase error metric or detector
2. Frequency-controllable oscillator
3. Loop filter

Loop "type" refers to the number of ideal poles (or integrators) within the linear system. A voltage-controlled oscillator (VCO) is an ideal integrator of phase for example.

Loop "order" refers to the polynomial order of the describing characteristic equation for the linear system. Loop-order must always be greater than or equal to the loop-type.

Although the term "settling time" is frequently used in the literature, a specified settling time is meaningless unless the definition for settling is also provided. A properly rigorous statement would be for example, "The settling time for the PLL is 1.5 msec to within ±5 degrees of steady-state phase."

Much more extensive discussion of PLL-related terminology is available in [3,4,12].

2.3 Continuous-Time Versus Discrete-Time Systems

PLL work was originally based upon continuous-time dynamics and engineers utilized the Laplace transform to mathematically describe linear PLL behavior. The world has however gone digital and with it, time has been discretized and dynamic quantities sampled. The connection between continuous-time and discrete-time systems can be easily bridged by making use of the Poisson Sum formula [3]. This formula relates the continuous-time function h(t) and its Fourier transform H(f) to the discretized world as

[1] http://www.globaltechnoscan.com/20thSep-26thSep/out_of_time.htm

[2] [3] Chapter 1

$$\textbf{(1)} \qquad \sum_k T_s h(kT_s)\exp(-j2\pi f\, kT_s) = \sum_m H\left(f \pm \frac{m}{T_s}\right)$$

where T_s is the time interval between samples. The left-hand side of (1) is by definition the z-transform of h(t) weighted by the quantity T_s.

It is insightful to look at this statement for the classic type-2 3rd-order PLL shown in Figure 1 for which the open-loop gain is given by

$$\textbf{(2)} \qquad G_{OL}(s) = \left(\frac{\omega_n}{s}\right)^2 \frac{1+s\tau_2}{1+s\tau_p}$$

Figure 1 Simple Charge-Pump PLL (Type-2, 3rd Order)

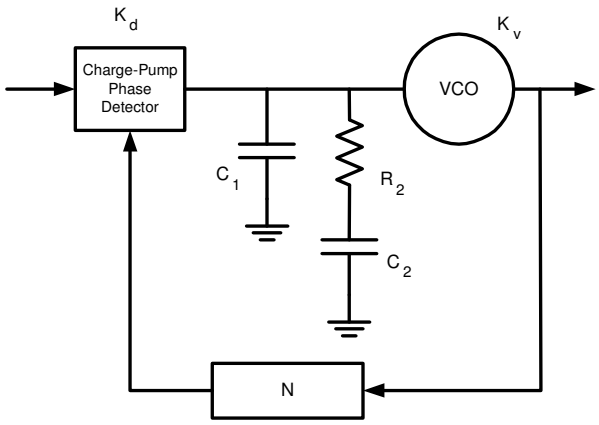

$$\textbf{(3)} \qquad \omega_n = \sqrt{\frac{K_d K_v}{N(C_1+C_2)}}$$

$$\textbf{(4)} \qquad \zeta = \frac{1}{2}\omega_n \tau_2$$

where

$$\textbf{(5)} \qquad \tau_2 = R_2 C_2$$

$$\textbf{(6)} \qquad \tau_p = \frac{C_1 C_2 R_2}{C_1 + C_2}$$

where K_v is the VCO tuning sensitivity (rad/ sec/ V), K_d is the phase detector gain (A/ rad.), N is the feedback divider ratio, and τ_p and τ_2 are the time constants associated with the lead-lag loop filter. In this form, the loop natural frequency and loop damping factor are given respectively by (3) and (4).

The discrete-equivalent z-transform for $G_{OL}(s)$ can be computed as

$$\textbf{(7)} \qquad G_{OL}(z) = \omega_n^2 Z\left[\frac{1+s\tau_2}{s^2(1+s\tau_p)}\right] = \omega_n^2\left[\frac{(\tau_2-\tau_p)z}{z-1} + \frac{zT_s}{(z-1)^2} + \frac{(\tau_p-\tau_2)z}{z-\exp\left(\frac{-T_s}{\tau_p}\right)}\right]$$

As developed at length in chapters 4 & 5 of [3], sampling control system factors adversely affect PLL stability, settling time and phase noise performance as the closed-loop bandwidth is permitted to exceed approximately 1/ 10 of the phase comparison frequency. Sampling effects on the open-loop and closed-loop transfer functions can be assessed by either going to the trouble to first compute the z-transform of the open-loop gain function as in (7), or the Poisson Sum formula can be used to compute the closed-loop transfer function much more conveniently as

$$\textbf{(8)} \qquad H(s) = \frac{G_{OL}(s)}{1 + \frac{1}{T_s}\sum_k G_{OL}\left(s + j\frac{2\pi k}{T_s}\right)}$$

Only a very few of the aliased $G_{OL}(s)$ gain terms need to be retained in the denominator in order to very accurately capture the sampling effects of interest.

The open-loop gain functions with and without the inclusion of sampling effects are shown in Figure 2 assuming a sampling rate of 100 kHz, a natural frequency of 5 kHz and damping factor of 0.90. The closed-loop response for this same system is shown in Figure 3 using (8).

Figure 2 Closed-Loop Gain Showing Continuous and Sampled Gain Forms[3]

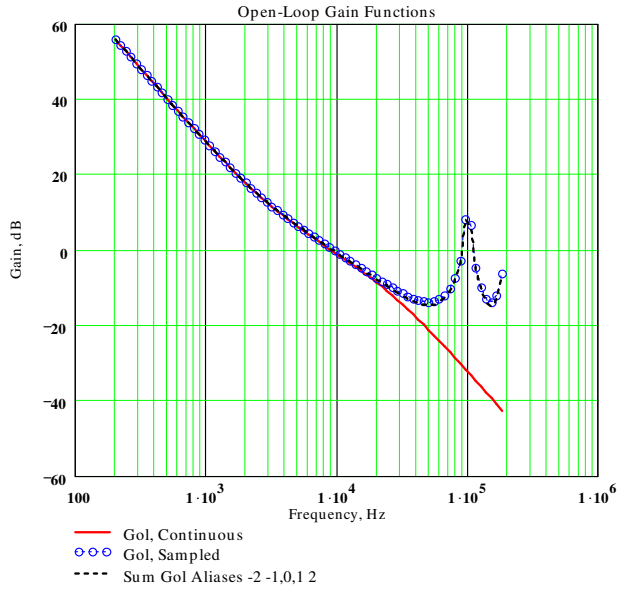

Figure 3 Closed-Loop Behavior for this case

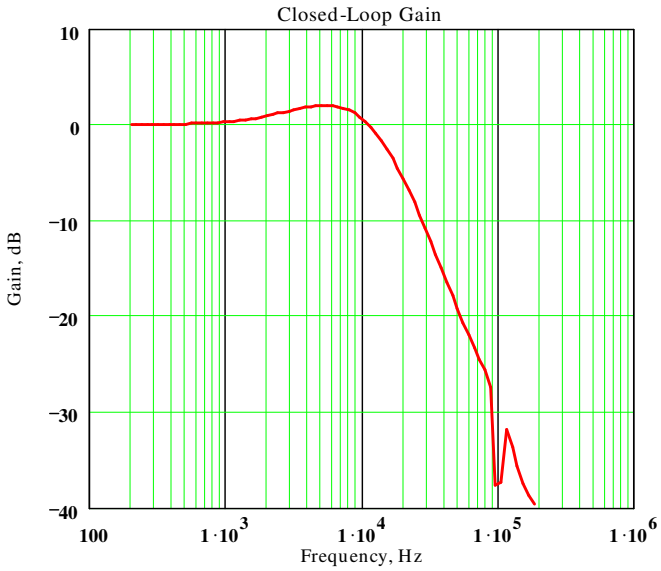

If the PLL natural frequency is increased to 12.5kHz (representing 1/ 8 of the sampling rate), stability problems become readily apparent is the excessive amount of gain-peaking that appears as shown in Figure 5 and the almost nonexistent gain-margin as shown in Figure 4.

Designers should be certain to address sampling effects as the percentage loop bandwidth (compared to the phase comparison frequency) is increased. Gain-peaking frequently degrades performance more than expected even though the system's stability margins are acceptable.

[3] Phase comparison frequency of 100 kHz assumed, natural frequency of 5 kHz, damping factor of 0.90

Figure 4 Open-Loop Gain for Increased PLL Bandwidth Case[4]

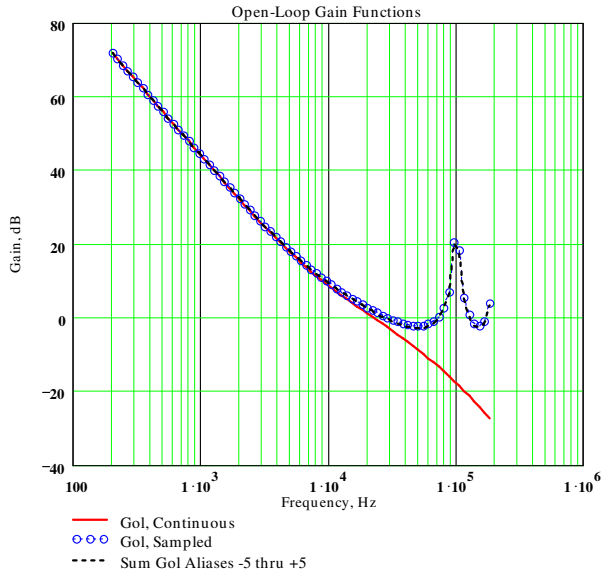

Figure 5 Closed-Loop Behavior for Increased PLL Bandwidth Case

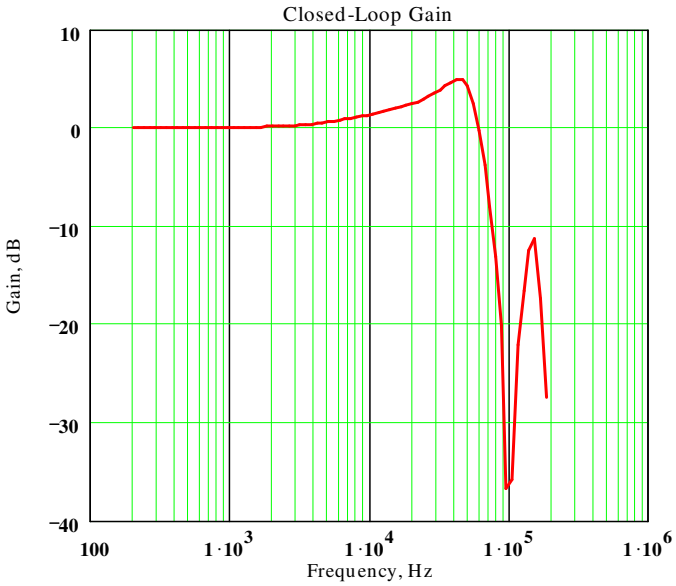

2.4 PLL Theory Perspectives

Phase-locked loop theory of operation can be looked at from several different perspectives. As we have just seen in the previous section, time-continuous and sampled system analysis of PLLs used for frequency synthesis produce almost identical results unless the closed-loop bandwidth becomes an appreciable fraction of the phase comparison frequency being used. In a similar fashion, different analysis must be used to study PLL operation under low signal-to-noise ratio (SNR) cases (e.g., customarily found in receiver applications) as compared to high SNR cases (e.g., like those encountered in frequency synthesizer usage). Several different perspectives that all help expand the phase-locked loop concept are discussed in the material that follows.

2.5 Control Theory Perspective (High SNR)

The control theory perspective of PLLs is normally the setting with which electrical engineers are dominantly familiar. Control theory concepts were used earlier in Section 2.3. Continuing in this vein, the classical type-2 second-order PLL that will be used for these discussions is shown in Figure 6. In our first view of this PLL in the strictly continuous-time domain, the phase detector is assumed to be linear (i.e., no sample-and-hold present).

Several first-order approximations are helpful to keep in mind when dealing with this classical PLL system based upon simple Bode diagramming techniques. The open-loop gain diagram of interest is Figure 7 whereas Figure 8 pertains to the closed-loop characteristics. In both figures, the unity-gain radian frequency ω_u is given by (11).

[4] Phase comparison frequency of 100 kHz assumed, natural frequency of 12.5kHz, damping factor of 0.90

Figure 6 Classical Type-2 Second-Order PLL with Sample-and-Hold Phase Detector

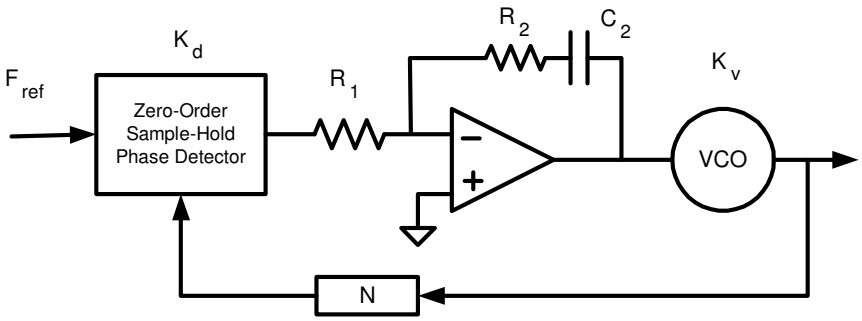

$$\omega_n = \sqrt{\frac{K_d K_v}{N\tau_1}} \quad \textbf{(9)}$$

$$\zeta = \frac{1}{2}\omega_n \tau_2 \quad \textbf{(10)}$$

$$\omega_u = \omega_n \sqrt{2\zeta^2 + \sqrt{4\zeta^4 + 1}} \quad \textbf{(11)}$$

Figure 7 Open-Loop Gain Approximations for Classic Type-2 PLL

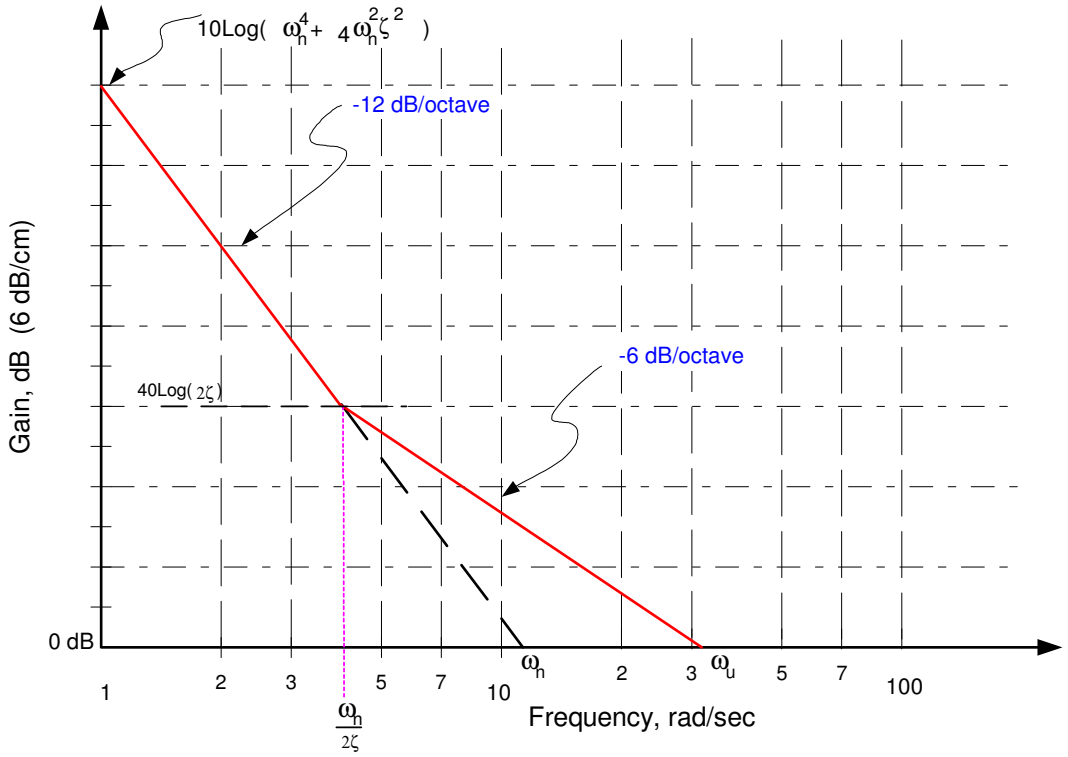

Figure 8 Closed-Loop Approximations for Classic Type-2 PLL

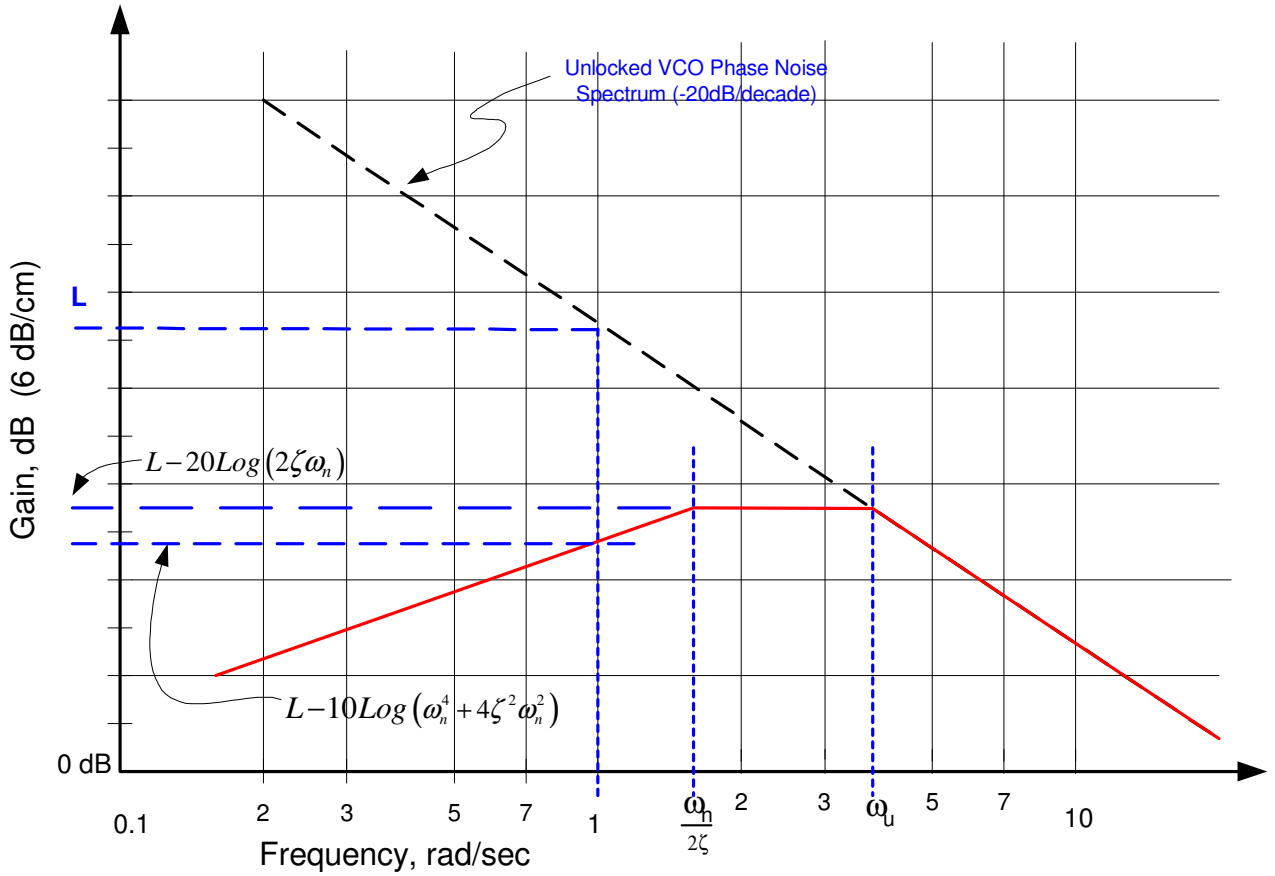

As noted elsewhere, the behavior of real-world sampled systems matches the continuous-time behavior very closely if the system bandwidths are small relative to the sampling rate. Therefore, it is very convenient to use the results from continuous-time theory to approximate useful quantities for both types of systems. A number of these helpful results for the continuous-time case are provided in Table 1.

Table 1 Helpful Formula for Classic Type-2 PLL Given by (12)[5] (ζ<1)

Description	Formula
Closed-Loop Unity-Gain Frequency	$F_{Closed-Loop\,0dB}=\frac{\sqrt{2}\omega_n}{2\pi}$ Hz
Closed-Loop Gain -3 dB Frequency	$F_{-3dBClosed}=\frac{\omega_n}{2\pi}\sqrt{1+2\zeta^2+2\sqrt{\zeta^4+\zeta^2+\frac{1}{2}}}$ Hz
Phase Margin	$\theta_{M\,\mathrm{arg}in}=\tan^{-1}\left(2\zeta\sqrt{2\zeta^2+\sqrt{4\zeta^4+1}}\right)$
Closed-Loop Maximum Gain-Peaking Frequency	$F_{Gain-Peak}=\frac{1}{2\pi}\frac{\omega_n}{2\zeta}\sqrt{\sqrt{1+8\zeta^2}-1}$ Hz

[5] NOTE: No sample-and-hold included for these results; i.e., strictly continuous-time PLL

Description	Formula
% Transient Overshoot in Frequency for Frequency Step	$T_{pk} = \frac{2}{\omega_n\sqrt{1-\zeta^2}}\tan^{-1}\left(\frac{\sqrt{1-\zeta^2}}{\zeta}\right)$ $OS_{\%} = \exp\left(-\zeta\omega_n T_{pk}\right)\left[\cos\left(\sqrt{1-\zeta^2}\,\omega_n T_{pk}\right) - \frac{\zeta}{\sqrt{1-\zeta^2}}\sin\left(\sqrt{1-\zeta^2}\,\omega_n T_{pk}\right)\right]\times 100\%$
Time of Peak Phase-Error Due to Step-Frequency Change	$T_{fstep} = \frac{1}{\omega_n\sqrt{1-\zeta^2}}\tan^{-1}\left(\frac{\sqrt{1-\zeta^2}}{\zeta}\right)$
Time of Peak Phase-Error Due to Step-Phase Change	$T_{\theta step} = \frac{1}{\omega_n\sqrt{1-\zeta^2}}\tan^{-1}\left(\frac{2\zeta\sqrt{1-\zeta^2}}{2\zeta^2-1}\right)$
Transient Response $\Delta F \rightarrow \theta(t)$	$\theta_{pd}(t) = \frac{2\pi\,\Delta F}{\omega_n}\frac{\exp\left(-\zeta\omega_n t\right)}{\sqrt{1-\zeta^2}}\sin\left(\omega_n\sqrt{1-\zeta^2}\,t\right)$
Transient Response $\Delta F \rightarrow f(t)$	$f_{pd}(t) = \Delta F\exp\left(-\zeta\omega_n t\right)\left[\cos\left(\omega_n\sqrt{1-\zeta^2}\,t\right) - \frac{\zeta}{\sqrt{1-\zeta^2}}\sin\left(\omega_n\sqrt{1-\zeta^2}\,t\right)\right]$
Transient Response $\Delta\theta \rightarrow \theta(t)$	$\theta_{pd}(t) = \Delta\theta\exp\left(-\zeta\omega_n t\right)\left[\cos\left(\omega_n\sqrt{1-\zeta^2}\,t\right) - \frac{\zeta}{\sqrt{1-\zeta^2}}\sin\left(\omega_n\sqrt{1-\zeta^2}\,t\right)\right]$
Transient Response $\Delta\theta \rightarrow f(t)$	$f_{pd}(t) = \frac{\Delta\theta\omega_n}{2\pi}\exp\left(-\zeta\omega_n t\right)\left[\frac{2\zeta^2-1}{\sqrt{1-\zeta^2}}\sin\left(\omega_n\sqrt{1-\zeta^2}\,t\right) - 2\zeta\cos\left(\omega_n\sqrt{1-\zeta^2}\,t\right)\right]$

In moving beyond the strictly continuous-time domain so that we can include digital dividers and phase detectors, we now include the zero-order sample-and-hold in the open-loop gain formula[6] as given by (12). In this formulation, K_d now has dimensions of V/ rad. And T_s is the time between sampling instants. The closed-loop natural frequency and damping factor are still given by (9) and (10) respectively.

(12)

$$G_{OL}(s) = \frac{1}{T_s}\left(\frac{1-e^{-sT_s}}{s}\right)\frac{K_d K_v}{N\tau_1}\frac{1+s\tau_2}{s^2} = \frac{1}{T_s}\left(\frac{1-e^{-sT_s}}{s}\right)\left(\frac{\omega_n}{s}\right)^2\left(1+2\zeta\frac{s}{\omega_n}\right)$$

In the case where the continuous-time open-loop gain is given by (12), full sampling effects can be included by computing the equivalent z-transform for this open-loop gain function which is

[6] Corresponds to Case 4 in [3]

(13) $$G_{OL}(z) = (\omega_n T_s)^2 \frac{z\left(\frac{1}{2} + \frac{\tau_2}{T_s}\right) + \left(\frac{1}{2} - \frac{\tau_2}{T_s}\right)}{(z-1)^2}$$

The system gain-margin G_M based upon (13) can be shown to be

(14) $$G_M = -20Log(\zeta \omega_n T_s)$$

but the gain margin is only defined provided that $\omega_n T_s < 4\zeta$. This same constraint applies for the system phase margin which is given in [3]. Since the z-domain (13) includes sampling effects whereas the Laplace s-domain (12) does not, the gain-margin predicted using the Laplace transform $G_{OL}(s)$ will always be more optimistic than actual as shown in Figure 9.

Figure 9 Gain Margin for Classic Type-2 PLL with Sample-and-Hold $\zeta = 0.707$

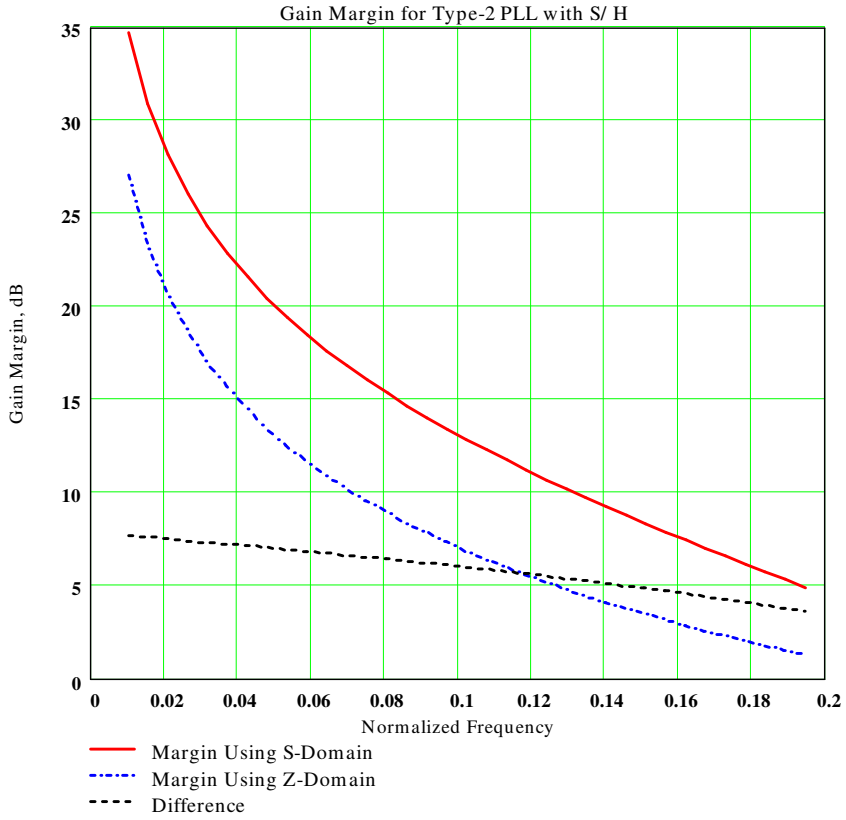

2.6 Phase-Locked Loops for Low SNR Applications

Low SNR applications are frequently observed at the receiving end of the system. The low SNR case can be cast in its most simple form as a simple sinusoidal signal immersed in additive white Gaussian noise (AWGN) and mathematically represented as

$$\textbf{(15)} \qquad r(t) = s(t) + n(t)$$

where s(t)= A cos($\omega_o t + \theta$) and the frequency and phase are considered constant. In the phase-lock condition, we can further assume that the frequency ω_o is known whereas the system is attempting to track the phase θ which is assumed to be quasi-static relative to the bandwidth of the PLL tracking system. It can be shown that the probability density function for the θ estimate can be written as

$$\textbf{(16)} \qquad p(\theta,\gamma) = \frac{\exp(-\gamma^2)}{2\pi}\left\{1 + \gamma\sqrt{\pi}\cos(\theta)\exp\left[\gamma^2\cos^2(\theta)\right]\left[1 + erf\left(\gamma\cos(\theta)\right)\right]\right\}$$

where γ is the receive SNR. The cumulative pdf using (16) can be numerically computed to create the traditional "S-curve" for the ideal phase error metric. Example probability density functions and their associated S-curves are shown in Figure 10 and Figure 11.

Fokker-Planck techniques can be used to solve the ensuing closed-loop tracking performance question for type-1 PLLs as provided in [10,11,12]. The classic result that follows is the well-known Tikhonov probability density function for the closed-loop phase error given as

$$\textbf{(17)} \qquad P(\phi) = \frac{\exp\left[\rho\cos(\phi)\right]}{2\pi I_o(\rho)}$$

where ρ is the SNR within the closed-loop bandwidth and $I_o()$ is the modified Bessel function of order zero. A more insightful exploration into the tracking performance of the type-1 PLL can be made by using the S-curve results that were just presented along with a first-order Markov model for the system.

In the first-order Markov model for a type-1 PLL [13,14], the phase error range $(-\pi,+\pi]$ is quantized across N states. Particularly nice closed-form results occur [14] if the state transitions are limited to strictly nearest-neighbor transitions as shown in Figure 12. Since the use of N states divides the total phase range of 2π into N equally-spaced phase intervals, the closed-loop bandwidth is inversely proportional to N. The state-transition probabilities denoted by the p_i and q_i are directly obtained from the S-curve at the SNR of interest.

Figure 10 Phase Error PDF

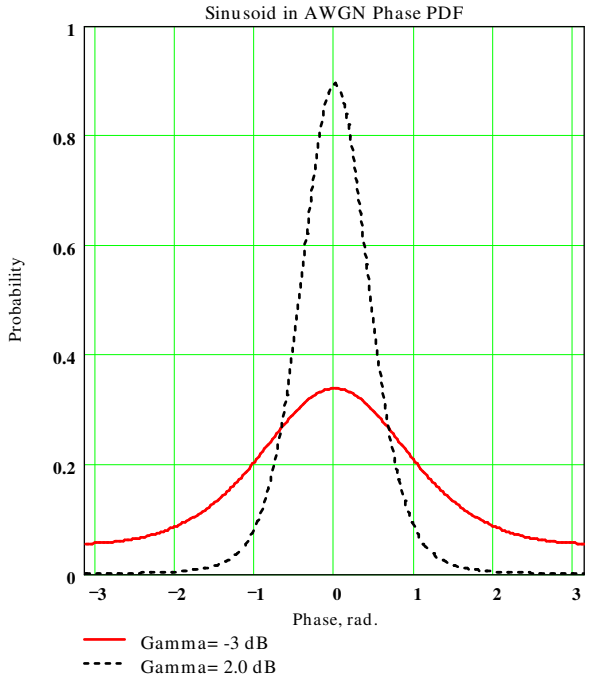

Figure 11 Cumulative Phase Error PDFs (S-Curves)

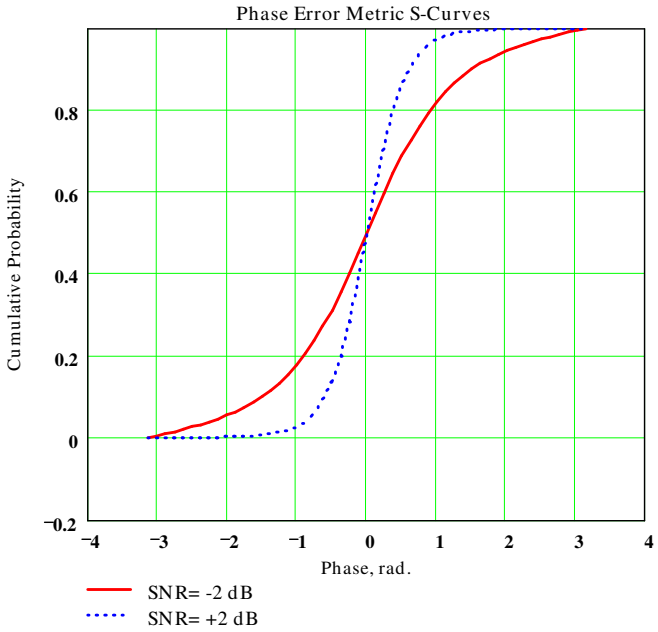

The Markov steady-state probability equations can be formulated as

(18) $S_1 = q_1 S_1 + q_2 S_2$

(19) $S_N = p_N S_N + p_{N-1} S_{N-1}$

(20) $S_k = p_{k-1} S_{k-1} + q_{k+1} S_{k+1}$

in which the S_k denote the steady-state occupancy probabilities for each state with k=1…N.

This set of equations can be solved as

(21) $$S_1 = \left\{ 1 + \sum_{k=2}^{N} \left[\prod_{i=1}^{k-1} \frac{p_i}{q_{i+1}} \right] \right\}^{-1}$$

(22) $$S_k = S_1 \prod_{i=1}^{k-1} \left(\frac{p_i}{q_{i+1}} \right) \text{ for k=2 to N.}$$

Figure 12 First-Order Markov Chain Model for Type-1 PLL

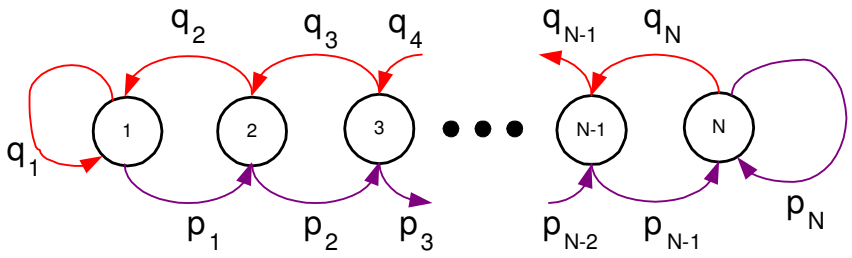

The mean tracking point and tracking error variance can be directly computed from the steady-state probabilities as

(23) $$\mu = \sum_{i=1}^{N} iS_i$$

(24) $$\sigma^2 = \sum_{i=1}^{N} (i-\mu)^2 S_i$$

The steady-state probabilities results are shown for two SNR cases with N=64 in Figure 13. The tracking error standard deviation for the SNR= -2dB case is 14.7 degrees rms whereas it is 9.9 degrees rms for the SNR= +2dB case.

Another important quantity related to low SNR PLL operation is the quantity known as "mean-time to cycle-slip". This can be directly computed from the transition probabilities in a similar fashion as described in [13,14].

Discrete modeling on the computer can be used to gain valuable insights without reverting to the complications of Fokker-Planck and Chapman-Kolmogorov equations for low-SNR performance investigations. Use of probability-mass methods can dramatically shorten analysis and simulation times.

Figure 13 Steady-State Probabilities

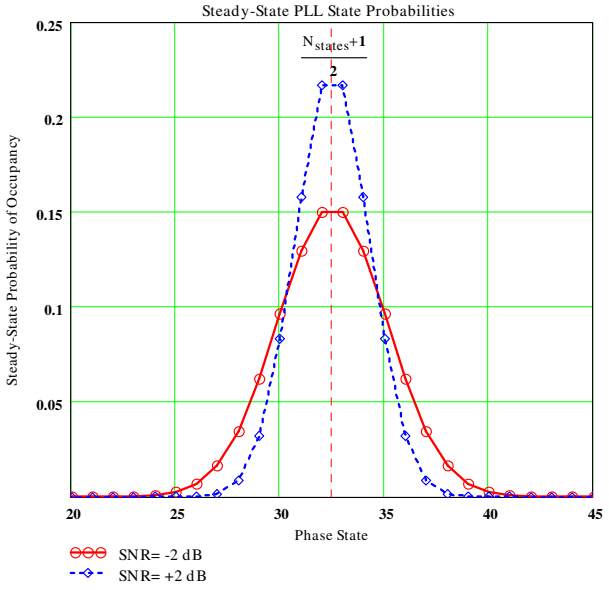

Figure 14 Tracking Error Standard Deviation (in degrees rms) and Effective Loop SNR[7] (dB) Versus Input SNR (dB)

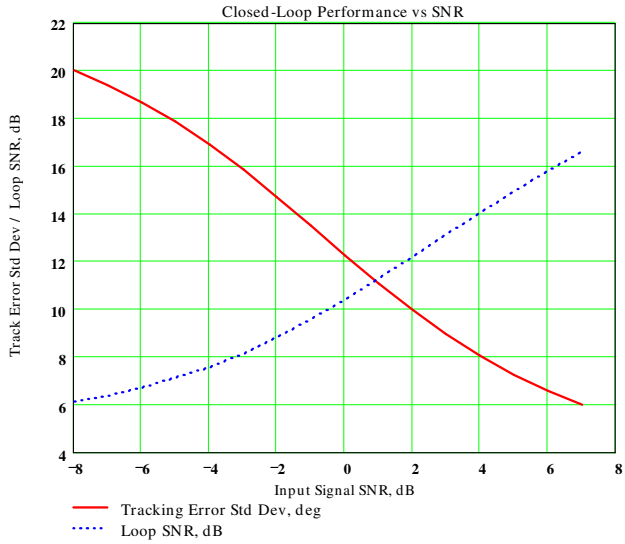

2.6.1 Minimum Variance Estimator

The design of a near-optimal PLL can be investigated by considering the phase-tracking problem as a minimum-variance estimation problem. Assume that we have a received signal that is represented by

$$r(t) = s(t) + n(t) \quad \textbf{(25)}$$

in which n(t) represents complex Gaussian channel noise and s(t) represents a complex sinusoid as

$$s(t) = A\exp\left[-j\omega_o t - j\theta\right] \quad \textbf{(26)}$$

If the received signal is discretized in time ($t_k = kT_s$), noise samples at t_k are assumed to be uncorrelated, and the estimates for the sinusoid's parameters are given by $\hat{A}, \hat{\omega}$ *and* $\hat{\theta}$, the variance for the joint estimate is given by

$$\sigma^2 = \sum_k \left| r(t_k) - \hat{A}\exp\left(-j\hat{\omega}t_k - j\hat{\theta}\right)\right|^2 \quad \textbf{(27)}$$

This can be expanded as

[7] Calculated using the approximation $\rho = \left(2\sigma^2_{track}\right)^{-1}$ where the tracking error variance is in radians^2.

$$\textbf{(28)} \quad \sigma^2 = \sum_k \left[\hat{A}^2 + \left| r(t_k) \right|^2 - 2\hat{A}\,\mathrm{Re}\left\{ r(t_k) \exp\left(j\hat{\omega} t_k + j\hat{\theta} \right) \right\} \right]$$

Assuming that the PLL has already achieved frequency-lock, we will assume that $\hat{\omega} = \omega_o$ and there is no frequency error present. Minimizing the estimator variance with respect to each individual parameter separately results in the following partial derivatives:

$$\textbf{(29)} \quad \frac{\partial \sigma^2}{\partial \hat{A}} = 2K\hat{A} - 2\sum_k \mathrm{Re}\left\{ r(kT) \exp\left(j\omega_o kT + j\hat{\theta} \right) \right\}$$

$$\textbf{(30)} \quad \frac{\partial \sigma^2}{\partial \hat{\theta}} = 2\hat{A}\sum_k \mathrm{Im}\left[r_k \exp\left(j\omega_o kT_s + j\hat{\theta} \right) \right]$$

where $\hat{A}$ is always a real quantity. The estimators that minimize the tracking error variance are then given as

$$\textbf{(31)} \quad \sum_k \mathrm{Im}\left[r_k z_k \exp\left(j\hat{\theta} \right) \right] = 0$$

$$\textbf{(32)} \quad \hat{A} = \frac{1}{K}\sum_k \mathrm{Re}\left[r_k z_k \exp\left(j\hat{\theta} \right) \right]$$

in which K is the total number of signal samples involved and $z_k = \exp(j\omega_o T_s)$. Although the estimator for $\hat{A}$ involves first knowing $\hat{\theta}$, no prerequisite knowledge of $\hat{A}$ is explicitly required in (31) in order to find the best phase estimate. The implementation structure suggested by (31) for the minimum-variance phase estimator is shown in Figure 15 [19].

Figure 15 Minimum-Variance Estimator Cast as a PLL

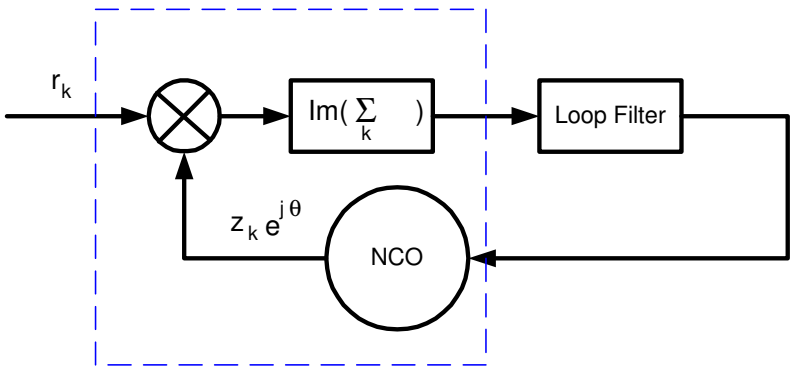

2.6.2 Maximum-Likelihood Estimator

Another estimator form can be derived based upon maximizing probability or what is called "likelihood" in estimation theory. In the case of a real sinusoid of unknown phase in real additive Gaussian noise similar to the situation we just examined, we seek to pick an estimate for θ that maximizes the probability

(33) $$P\left(\underset{\rightarrow}{r}\right)=(2\pi)^{-\frac{K}{2}}\left|R\right|^{-\frac{1}{2}}\exp\left\{-\frac{1}{2}\left[\underset{\rightarrow}{r}-\underset{\rightarrow}{s}\right]^{T}R^{-1}\left[\underset{\rightarrow}{r}-\underset{\rightarrow}{s}\right]\right\}$$

where $\underset{\rightarrow}{r}$ and $\underset{\rightarrow}{S}$ represent the K-dimensional measurement and signal estimate, and R is the KxK correlation matrix. In this real case being considered, $s_k = A\cos(\omega_o k T_s+\theta)$. We can equivalently seek to maximize the log-likelihood function of θ which is given by

(34) $$L(\theta)=-\frac{K}{2}\log(2\pi)-\frac{1}{2}\log\left(\left|R\right|\right)-\frac{1}{2}\left[\left(\underset{\rightarrow}{r}-\underset{\rightarrow}{s}\right)^{T}R^{-1}\left(\underset{\rightarrow}{r}-\underset{\rightarrow}{s}\right)\right]$$

Assuming that the noise samples have equal variances and are uncorrelated, $R=\sigma_n^2 I$ where I is the KxK identity matrix. In order to maximize (34) with respect to θ, a necessary condition is that the derivative of (34) with respect to θ be zero, or equivalently

(35) $$\begin{aligned}\frac{\partial L}{\partial\theta}&=\frac{\partial}{\partial\theta}\sum_k\left[r_k-A\cos(\omega_o t_k+\theta)\right]^2=0\\&=\sum_k 2\left[r_k-A\cos(\omega_o t_k+\theta)\right]A\sin(\omega_o t_k+\theta)=0\end{aligned}$$

Simplifying this result further and discarding the double-frequency terms that results, the maximum-likelihood estimate for θ is that value that satisfies the constraint

(36) $$\overline{\sum_k r_k\sin\left(\omega_o t_k+\hat{\theta}\right)}=0$$

The top-line indicates that double-frequency terms are to be filtered out and discarded. This result is equivalent to the minimum-variance estimator derived earlier in (31).

Under the assumed linear Gaussian assumptions, the minimum-variance (MV) and maximum-likelihood (ML) estimators take the same form when implemented with a PLL. Both algorithms seek to reduce any quadrature error to zero.

3 Summary

Diverse design perspectives can be utilized to improve and extend our basic understanding of the PLL concept. Mathcad worksheets for most of the results presented in this paper can be found at. http://www.siliconrfsystems.com/design_notes.htm .

In the second part of this article, we will close out the theoretical discussions by looking at (i) the maximum a posteriori (MAP) estimator PLL form, (ii) the Cramer-Rao bound which provides helpful insights into achievable theoretical performance, and finally (iii) the PLL derived based upon Kalman filtering concepts. The balance of the article will look at several real-world applications using the PLL concept.

4 Bibliography

1. de Bellescize, H., "La Reception Synchrone,", *Onde Electr*, Vol. 11, June 1932, pp. 230-240
2. Sepe, R.B., R.I. Johnston, "Frequency Multiplier and Frequency Waveform Generator," U.S. Patent No. 3,551,826, December 29, 1970
3. Crawford, J.A., Frequency Synthesizer Design Handbook, Artech House, 1994
4. Gardner, F.M., *Phaselock Techniques*, 2nd Ed., John Wiley & Sons, 1979
5. Best, R.E., Phase-Locked Loops Theory Design & Applications, McGraw-Hill Book, 1984
6. Adler, R., "A Study of Locking Phenomena in Oscillators," Proc. IRE, June 1946
7. Kurokawa, K., "Injection Locking of Microwave Solid-State Oscillators," Proc. IEEE, Oct. 1973
8. Dewan, E.M., "Harmonic Entrainment of van der Pol Oscillations: Phaselocking and Asynchronous Quenching," IEEE Trans. Automatic Control, Oct. 1972
9. Uzunoglu, V., White, M.H., "Synchronous and the Coherent Phase-Locked Synchronous Oscillators: New Techniques in Synchronization and Tracking," IEEE Trans. Cir, & Sys., July 1989
10. Blanchard, A., *Phase-Locked Loops Application to Coherent Receiver Design*, John Wiley & Sons, 1976
11. Van Trees, H., *Detection, Estimation and Modulation Theory*, Part II, John Wiley & Sons
12. Egan, W.F., *Phase-Lock Basics*, John Wiley & Sons, 1998
13. Holmes, J.K., *Coherent Spread Spectrum Systems*, John Wiley & Sons, 1982
14. Holmes, J.K., "Performance of a First-Order Transition Sampling Digital Phase-Locked Loop Using Random-Walk Models," IEEE Trans. Comm., April 1972
15. Viterbi, A.J., *Principles of Coherent Communication*, McGraw-Hill
16. Meyr, H., et al., *Digital Communication Receivers Synchronization, Channel Estimation, and Signal Processing*, John Wiley & Sons, 1998
17. Srinath, M.D., Rajasekaran, P.K., *An Introduction to Statistical Signal Processing with Applications*, John Wiley & Sons, 1979
18. Lindsey, W.C., Simon, M. K., *Telecommunication Systems Engineering*, Prentice-Hall, 1973
19. Ziemer, R.E., Peterson, R.L., *Digital Communications and Spread Spectrum Systems*, Macmillan, 1985
20. Scharf, L.L., Statistical Signal Processing Detection, Estimation, and Time Series Analysis, Addison-Wesley, 1991

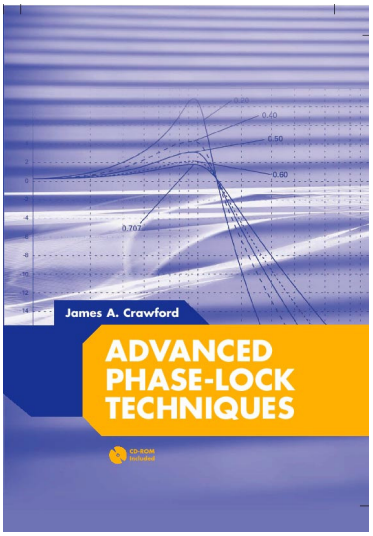

Advanced Phase-Lock Techniques

James A. Crawford

2008

Artech House

510 pages, 480 figures, 1200 equations
CD-ROM with all MATLAB scripts

ISBN-13: 978-1-59693-140-4
ISBN-10: 1-59693-140-X

Chapter	Brief Description	*Pages*
1	*Phase-Locked Systems—A High-Level Perspective* An expansive, multi-disciplined view of the PLL, its history, and its wide application.	26
2	*Design Notes* A compilation of design notes and formulas that are developed in details separately in the text. Includes an exhaustive list of closed-form results for the classic type-2 PLL, many of which have not been published before.	44
3	*Fundamental Limits* A detailed discussion of the many fundamental limits that PLL designers may have to be attentive to or else never achieve their lofty performance objectives, e.g., Paley-Wiener Criterion, Poisson Sum, Time-Bandwidth Product.	38
4	*Noise in PLL-Based Systems* An extensive look at noise, its sources, and its modeling in PLL systems. Includes special attention to 1/*f* noise, and the creation of custom noise sources that exhibit specific power spectral densities.	66
5	*System Performance* A detailed look at phase noise and clock-jitter, and their effects on system performance. Attention given to transmitters, receivers, and specific signaling waveforms like OFDM, M-QAM, M-PSK. Relationships between EVM and image suppression are presented for the first time. The effect of phase noise on channel capacity and channel cutoff rate are also developed.	48
6	*Fundamental Concepts for Continuous-Time Systems* A thorough examination of the classical continuous-time PLL up through 4^{th}-order. The powerful Haggai constant phase-margin architecture is presented along with the type-3 PLL. Pseudo-continuous PLL systems (the most common PLL type in use today) are examined rigorously. Transient response calculation methods, 9 in total, are discussed in detail.	71
7	*Fundamental Concepts for Sampled-Data Control Systems* A thorough discussion of sampling effects in continuous-time systems is developed in terms of the *z*-transform, and closed-form results given through 4^{th}-order.	32
8	*Fractional-N Frequency Synthesizers* A historic look at the fractional-N frequency synthesis method based on the U.S. patent record is first presented, followed by a thorough treatment of the concept based on Δ-Σ methods.	54
9	*Oscillators* An exhaustive look at oscillator fundamentals, configurations, and their use in PLL systems.	62
10	*Clock and Data Recovery* Bit synchronization and clock recovery are developed in rigorous terms and compared to the theoretical performance attainable as dictated by the Cramer-Rao bound.	52